IJFAC

Indonesian Journal of
Fundamental and Applied Chemistry

Article http://ijfac.unsri.ac.id

Modification of Activated Carbon from Palm Kernel Shells with Fe_3O_4 Magnetic for Water Treatment of Enim River

Damayanti Damayanti[1], Susila Arita[2] and Poedji Loekitowati Hariani[3*]

[1] Magister Program of Chemical Engineering Department, Faculty of Engineering, Universitas Sriwijaya, Jalan Palembang Prabumulih Km. 32 Indralaya, Ogan Ilir
[2] Chemical Engineering Department, Faculty of Engineering, Universitas Sriwijaya, Jalan Palembang Prabumulih Km. 32 Indralaya, Ogan Ilir
[3] Department of Chemistry, Faculty of Mathematics and Natural Science, Universitas Sriwijaya, Jalan Palembang Prabumulih Km. 32 Indralaya, Ogan Ilir

*Corresponding Author: puji_lukitowati@mipa.unsri.ac.id

Abstract

The economical, easy-to-implement, and regenerative treatment methods are essential to obtain clean water. In this study, activated carbon was synthesized from palm kernel shells using $ZnCl_2$ as an activator. The activated carbon was then modified with Fe_3O_4. The resulting activated carbon and activated carbon-Fe_3O_4 product were characterized using XRD, SEM-EDX, VSM, and BET surface area analysis. Furthermore, activated carbon-Fe_3O_4 was applied to reduce Fe ions, turbidity, and total suspended solids (TSS) and increase the pH value in Enim river water. The resulting activated carbon has met SNI standards, with a moisture content of 8.81%, ash content of 5.475%, and an iodine adsorption capacity of 1763.86 mg/L. The synthesized activated carbon-Fe_3O_4 exhibits strong magnetic properties, with a saturation magnetization value of 68.82 emu/g and a surface area of 355.42 m^2/g. Optimal conditions for the treatment of Enim river water were obtained at an adsorbent dose of 40 mg/L, a stirring rate of 120 rpm, and a stirring time of 120 minutes. Under these conditions, the Fe ion reduction efficiency reached 96.95%, turbidity 89.83%, and TSS 80.74%, while the pH increased from 6.23 to 6.74. FTIR analysis showed a change in peak intensity in the activated carbon-Fe_3O_4 after the adsorption process, indicating interaction with contaminants. The adsorption process of Fe ions by activated carbon-Fe_3O_4 follows a pseudo-second-order kinetic model.

Keywords: *palm kernel shells, activated carbon, Fe_3O_4, turbidity, total suspended solid*

Article Info

Received 7 August 2025
Received in revised 10 September 2025
Accepted 10 September 2025
Available Online 29 October 2025

Abstrak (Indonesian)

Metode pengolahan yang ekonomis, mudah diterapkan, dan memungkinkan untuk diregenerasi sangat diperlukan untuk mendapatkan air bersih. Pada penelitian ini, disintesis karbon aktif dari cangkang kelapa sawit menggunakan $ZnCl_2$ sebagai aktivator. Karbon aktif kemudian dimodifikasi dengan Fe_3O_4. Karbon aktif-Fe_3O_4 yang dihasilkan dikarakterisasi menggunakan XRD, SEM-EDX, VSM, dan BET. Selanjutnya karbon aktif-Fe_3O_4 diaplikasikan untuk menurunkan konsentrasi ion Fe, kekeruhan, dan total padatan tersuspensi, serta meningkatkan nilai pH pada air Sungai Enim. Hasil penelitian menunjukkan karbon aktif telah memenuhi standar SNI, dengan kadar air sebesar 8,81%, kadar abu 5,475%, dan kapasitas adsorpsi terhadap iodium mencapai 1763,86 mg/L. Karbon aktif-Fe_3O_4 hasil sintesis memiliki sifat magnetik yang kuat, dengan nilai saturation magnetization sebesar 68,82 emu/g dan luas permukaan sebesar 355,42 m^2/g. Kondisi optimal untuk pengolahan air sungai Enim diperoleh pada dosis adsorben 40 mg/L, kecepatan pengadukan 120 rpm, dan lama pengadukan selama 120 menit. Dalam kondisi ini, efisiensi penurunan konsentrasi ion Fe mencapai 96,95%, kekeruhan 89,83%, dan total padatan tersuspensi 80,74%, sementara pH meningkat dari 6,23 menjadi 6,74.

Analisis FTIR menunjukkan adanya perubahan intensitas puncak pada karbon aktif-Fe_3O_4 setelah proses adsorpsi, yang mengindikasikan interaksi dengan kontaminan. Proses adsorpsi ion Fe oleh karbon aktif-Fe_3O_4 mengikuti model kinetika pseudo-orde dua.

Kata Kunci: Cangkang kelapa sawit, karbon aktif, Fe_3O_4, ion Fe, kekeruhan, padatan terlarut

INTRODUCTION

The availability of clean water for both households and industry is an indicator of a country's development level [1,2]. Health issues are related to drinking water quality. Efficient treatment technologies must meet several criteria, including ease of operation, low investment, operational, and maintenance costs, and effectiveness in improving water quality [3,4].

Several methods have been used to improve the quality of raw water for drinking water sources, including filtration using natural materials such as grass to reduce turbidity in lake water [5], adsorption of heavy metal ions from rivers using fruit waste [6], the use of polyaluminum chloride as a coagulant to reduce turbidity in dammed surface water [7], and the reduction of Total Suspended Solid (TSS) and Total Dissolved Solid (TDS) from peat water using ceramic membranes made from sand and sawdust [8].

Raw water treatment for drinking water sources often uses coagulation/flocculation coagulants such as aluminum sulfate or alum ($Al_2(SO_4)_3 \cdot 14H_2O$), which are the most widely used coagulants due to their high efficiency and low cost [9,10]. The use of aluminum sulfate ($Al_2(SO_4).12H_2O$) has the disadvantage of affecting the taste and odor of water, the formation of hydrogen sulfide and volatile organic sulfur compounds, causing unpleasant odors [11,12]. In addition, exposure to aluminum sulfate can cause toxic effects on various organ systems, including the central nervous system, respiratory, skeletal, hematopoietic, reproductive, digestive, and integumentary, potentially causing conditions such as neurodegenerative diseases, osteomalacia, and cognitive disorders [13,14].

The Enim river, located in Muara Enim Regency, is known as one of the largest rivers in South Sumatra. The community typically uses the river's water for household needs. Furthermore, the Enim river serves as a raw water source to meet the clean water needs of the Muara Enim Regency community, managed by the Muara Enim Regency Regional Water Company (PDAM), a Regionally-Owned Enterprise (BUMD). The PDAM uses aluminum sulfate as a coagulant to reduce the turbidity and color of the raw water.

Activated carbon is an adsorbent with a large specific surface area, high pore volume, good chemical stability, high thermal stability, low production costs, and ease of regeneration. It can be made from agricultural waste [15,16]. Other researchers have demonstrated the effectiveness of activated carbon for raw drinking water treatment. For example, activated carbon derived from bamboo (BAC) and coconut shell (CSAC) has significantly reduced TSS. In a test using 750 mL of river water, 10 g of BAC was able to eliminate 83.35% of TSS and 82.61% of NH_3-N, whereas 10 g of CSAC removed 79.18% of TSS and 83.73% of NH_3-N [17].

Palm kernel shells are an abundant agricultural waste product. Palm oil is produced primarily in Southeast Asian countries such as Indonesia, Malaysia, and Thailand [18]. Several researchers have used activated carbon as an adsorbent, including to absorb phenol with an effectiveness of 87% [19] and the dye methylene blue with an efficiency of 99.6% [20].

In its application, activated carbon has weaknesses in terms of separation and regeneration. Furthermore, the addition of Fe_3O_4 can improve thermal and chemical stability [21,22]. Magnetite (Fe_3O_4) has high magnetic properties, high biocompatibility, is easily separated using an external magnetic field, and is relatively low-cost [23].

In this study, activated carbon was synthesized from palm kernel shells modified with Fe_3O_4. The quality of the activated carbon was compared with the Indonesian National Standard (SNI) [24]. Characterization of activated carbon and activated carbon-Fe_3O_4 was carried out using XRD, SEM-EDS, VSM, and BET surface area. Furthermore, activated carbon-Fe_3O_4 was used to reduce Fe ions, turbidity, TSS, and improve pH.

MATERIALS AND METHODS

Material

Palm kernel shells were collected from a palm oil industry in Muara Enim. River water samples were from the Enim river, Muara Enim, regency. Other materials included $ZnCl_2$, HCl, iodine, $FeCl_3$, and $FeCl_2$ from Merck, Germany. Distilled water and demineralized water were used for reagent preparation and washing.

Preparation of Activated Carbon

The production process begins by cleaning palm shells to remove any impurities, followed by washing with distilled water and drying at 105 °C for 24 h. The

dried shells are then ground to a fine powder passing through a 140-mesh sieve. Carbonization is conducted at 700 °C for a duration of 3 h. Subsequently, 100 g of the resulting char is impregnated with 200 mL of a 1 M $ZnCl_2$ solution and stirred at 85 °C for 3 h. The impregnated material undergoes calcination at 500 °C for 3 h. Afterward, the activated carbon is thoroughly rinsed with distilled water and 0.1 M HCl until a neutral pH is achieved. The final drying step is performed at 105 °C for 2 h [25,26]. The quality of the activated carbon is then evaluated based on moisture content, ash content, and iodine number following SNI standards.

Synthesis of activated carbon-Fe_3O_4

Activated carbon-Fe_3O_4 was synthesized using the coprecipitation method, with a mass ratio of activated carbon: Fe_3O_4 = 2:1 [27]. A total of 10 g of activated carbon was added to 50 mL of a solution containing 2.79 g of $FeCl_2$ and 7.14 g of $FeCl_3$. The mixture was stirred while supplied with nitrogen gas, then gradually added 1 M NaOH solution until the pH was ± 11. The precipitate obtained was washed with distilled water until neutral. Finally, it was dried in an oven at 105 °C for 2 h.

Material characterization

Activated carbon and activated carbon-Fe_3O_4 were characterized using XRD (Shimadzu 7000) to identify the crystal phase, SEM-EDX (JEOL JSM-6510LA) to identify the morphology and elemental composition, BET surface area (Quantachrome Quadrasorb EVO) to determine the specific surface area, and magnetic properties were analyzed using VSM (Oxford Instruments). FTIR (Perkin-Elmer UATR) to identify functional groups before and after adsorption. Fe ion concentration was determined using AAS (Shimadzu AA-7800), turbidity using a turbidimeter (TU900), and TSS using a TSS meter (Hanna Instruments, 750W).

Adsorption Experiment

In this study, the effect of various variables, such as adsorbent dosage (10-50 mg/L), stirring speed (80-160 rpm), and stirring time (30-180 min), on the effectiveness of reducing Fe ion concentration, turbidity, and TSS, as well as changes in solution pH, was studied. The volume of river water used was 50 mL. Adsorption effectiveness was calculated using the formula:

$$\text{Removal (\%)} = \frac{(C_0 - C_t)}{C_0} \times 100 \quad (1)$$

where C_o and C_t are the initial concentration and the concentration at any time

RESULTS AND DISCUSSION

Activated Carbon Quality

Table 1 presents the quality analysis results of activated carbon derived from palm shell. All three parameters—moisture content, ash content, and iodine adsorption capacity meet the standard criteria for activated carbon. High moisture and ash content reduced effectiveness because some carbon pores may be occupied. Iodine adsorption is an important parameter for assessing the adsorption capacity of activated carbon for small molecules, which is directly related to the surface area and number of micropores. A high iodine value indicates that activated carbon can be used for water purification, gas treatment, and the adsorption of organic and inorganic materials [28].

Table 1. Activated carbon quality

Parameters	Result	SNI 06-3730-1995
Moisture Content	8.81%	≤ 15%
Ash Content	5.47%	≤ 10%
Iodine Adsorption Capacity	1763.86 mg/g	750 mg/g

Characterization of materials

The phase structure of activated carbon and activated carbon-Fe_3O_4 determined using XRD is presented in **Figure** 1. Two main peaks in activated carbon are at 2θ = 24.3° and 43.8°, which are characteristic of amorphous carbon with weak diffraction intensity. These peaks depict the crystal planes (002) and (100) according to JCPDS No. 41-1487 [21,29]. The presence of Fe_3O_4 in the activated carbon-Fe_3O_4 composite is confirmed by the appearance of sharp diffraction peaks at 2θ values of 2θ at 30.3°, 35.6°, 43.3°, 53.8°, 57.3° and 62.8° corresponding to the cubic crystal structure of Fe_3O_4 with crystal planes (220), (311), (400), (422), (511) and (440) (JCPDS No. 19-0629) [27,30]. The presence of Fe_3O_4 peaks confirms the successful impregnation of Fe_3O_4 into the activated carbon matrix, resulting in a composite with strong magnetic behavior.

SEM analysis was used to observe the surface morphology, while EDX was used to identify the composition of the constituent elements. **Figure** 2 presents the morphology of activated carbon and activated carbon modified with Fe_3O_4. It can be seen that activated carbon has a porous structure, the emergence of these pores can be caused by the effect of dehydration of the activator [21]. Impregnation of Fe_3O_4 on activated carbon shows that Fe_3O_4 particles are partially distributed on the surface, and the rest penetrate the pores of the activated carbon.

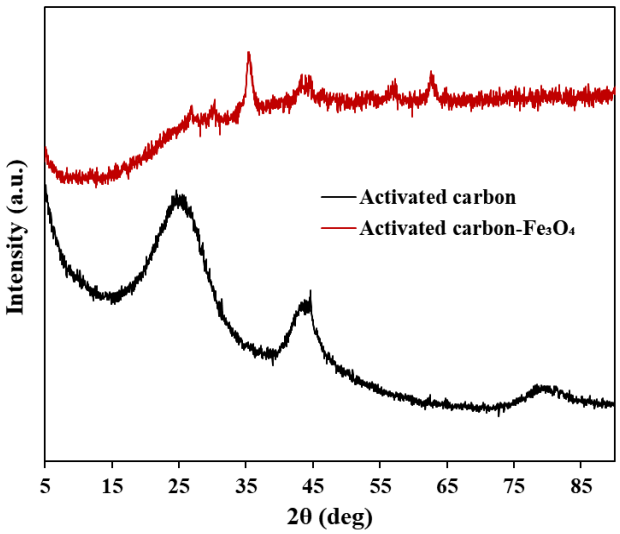

Figure 1. XRD patterns of activated carbon and activated carbon-Fe_3O_4

The activated carbon composition consists of 98% C and 2% oxygen. This carbon composition is greater than that of activated carbon from banana waste, which is 91.07% [31]. Evidence that the synthesis of activated carbon-Fe_3O_4 was successful is the presence of the Fe element of 37% and the reduction of the C element (37%) (**Figure** 3). This happens as Fe_3O_4 attaches to and partially masks the surface of the activated carbon.

The surface area of activated carbon and activated carbon-Fe_3O_4 is presented in **Table** 2**.** The surface area of activated carbon is 355.42 m^2/g, while that of activated carbon-Fe_3O_4 is 334.15 m^2/g. This decrease in surface area is due to some of the pores being filled by Fe_3O_4 [27,30]. The same phenomenon is that activated carbon from rice straw impregnated with Fe_3O_4 has a decrease in surface area from 204.69 m^2/g to 109.89 m^2/g [21]. The pore diameter of activated carbon and activated carbon-Fe_3O_4 is classified as mesopore in the range of 2-50 nm [32].

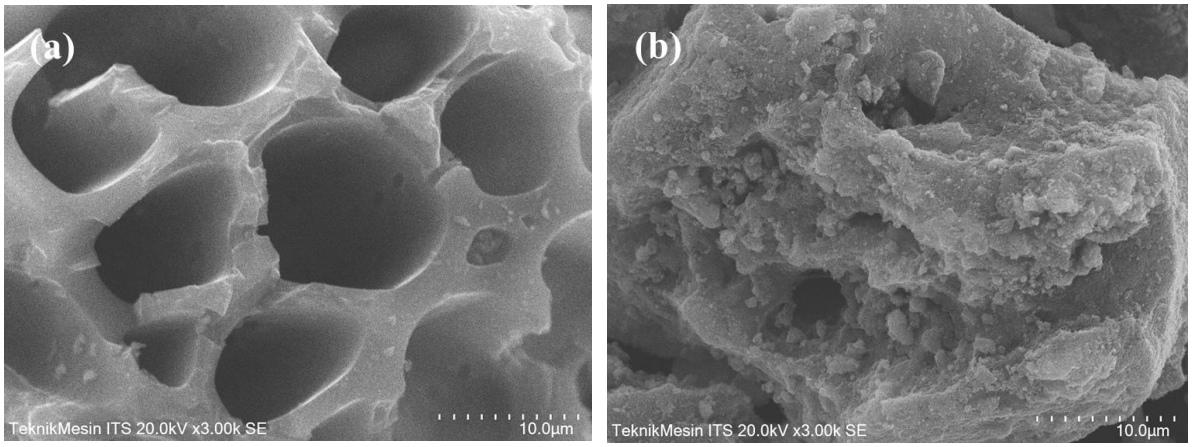

Figure 2. SEM image of (a) activated carbon and (b) activated carbon-Fe_3O_4

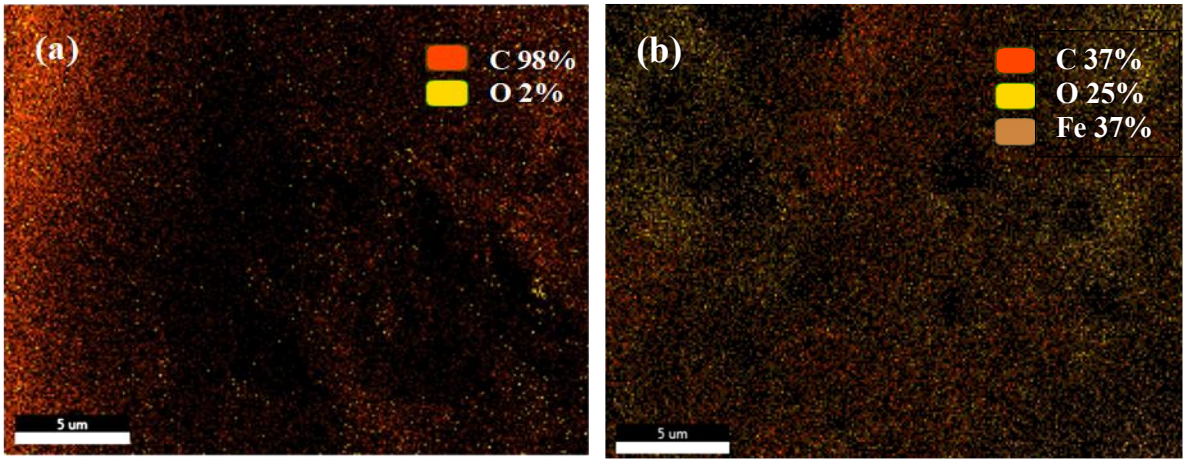

Figure 3. Energy dispersive X-ray (EDX) mapping analysis of (a) activated carbon and (b) activated carbon-Fe_3O_4

Table 2. Surface area of activated carbon and activated carbon-Fe_3O_4

Materials	BET surface area (m^2/g)	Pore diameter (nm)	Pore volume (cm^3/g)
Activated carbon	355.42	12.6	0.32
Activated carbon-Fe_3O_4	334.15	14.1	0.58

Activated carbon–Fe_3O_4 is magnetic due to the presence of Fe_3O_4 particles, which are ferromagnetic or superparamagnetic materials. When Fe_3O_4 is impregnated into the activated carbon, the resulting composite will inherit the magnetic properties of Fe_3O_4. These particles can be on the surface or in the pores of the activated carbon. As long as the amount and distribution are sufficient, the magnetic moment of Fe_3O_4 remains dominant, so the entire composite is magnetic.

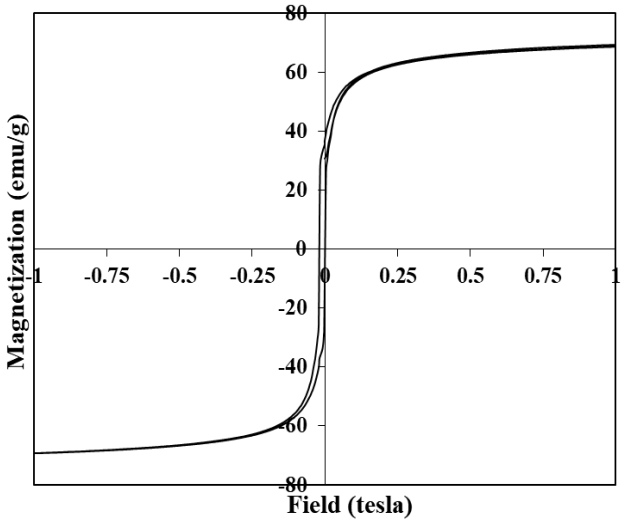

Figure 4. Magnetic hysteresis loops of activated carbon-Fe_3O_4

Figure 4 shows the magnetic moment value of activated carbon–Fe_3O_4 [23,30]. In this study, the magnetic moment value was 68.82 emu/g. This result is greater than activated carbon (from oak wood)–Fe_3O_4 of 43.81 emu/g [33] and activated carbon (vine shoots)– Fe_3O_4 of 30.43 emu/g [23]. This magnetic characteristic enables the easy separation of activated carbon-Fe_3O_4 from the solution following the adsorption process.

Adsorption experiment

The concentration of Fe ions, turbidity, TSS, and pH in the Enim river are 6.14 mg/L, 53.57 NTU, 1122 mg/L, and 6.23. The water standard as drinking water according to WHO, namely Guidelines for Drinking-water Quality [34], several parameters exceed the quality standard, namely Fe concentration (max 0.3 mg/L), and turbidity (<5 NTU), pH meets the quality standard (6.5-8.5), while TSS is not listed in the quality standard. The quality standard of river water as raw water for drinking water for TSS according to the regulation of the Governor of South Sumatra No. 16 of 2005, is listed as a maximum of 50 mg/L [35].

In this study, the effect of dosage was carried out with variations of 10, 20, 30, 40, and 50 mg/L as shown in **Figure** 5(a). Increasing the dosage increased the effectiveness of reducing the concentration of Fe ions, Turbidity, and TSS. At small doses, it is less effective in removing pollutants. When the dosage is minimal, there may not be enough adsorption sites on the surface of the activated carbon-Fe_3O_4 to capture and remove contaminants [29]. Optimum effectiveness occurs at a dose of 40 mg/L. Excessive dosages do not cause an increase in adsorption, it is possible that at higher doses a saturation point may be reached where the available active sites are adequately utilized, and further dose increases do not proportionally increase the removal rate [21,29].

The effect of stirring speed shows that the optimum removal conditions for Fe ions, Turbidity, and TSS were achieved at 120 minutes as shown in **Figure** 5(b). These results indicate that slower stirring rates are associated with less efficient pollutant removal. The limitation of stirring caused by this stirring rate can result in inadequate dispersion and mixing of the adsorbent in the effluent. As a result, the adsorbent may not come into effective contact with the pollutant, leading to lower removal rates. After the optimum conditions, the adsorbent may become unstable or over-dispersed without having time to capture the contaminant [29].

Figure 5(c) shows the effect of stirring time on the removal of Fe ion, turbidity, and TSS. At a stirring time of 30 minutes, the removal of Fe ion concentration, turbidity, and TSS was 81.10%, 72.86%, and 67.56%, respectively. Increasing stirring time was accompanied by increased contaminant removal until equilibrium was reached. Optimum conditions were achieved at 120 minutes with efficiencies of 96.95%, 89.83%, and 80.74%. Equilibrium conditions may have been reached, resulting in the highest removal rates. Interestingly, after the optimum time, there was a decrease in removal (%) for Fe ion, turbidity, and TSS. This may be due to saturation of active sites, desorption, or the formation of aggregates [29,36].

Figure 6 compares reductions of Fe ions, turbidity, TSS removal, and pH changes under optimum conditions, namely a dose of 40 mg/L, a

stirring speed of 120 rpm, and a stirring time of 120 minutes, using activated carbon and activated carbon-Fe_3O_4. It appears that activated carbon-Fe_3O_4 can reduce Fe ions better than activated carbon. The reduction of turbidity and TSS is through a precipitation or coagulation mechanism, not just adsorption. Activated carbon-Fe_3O_4 has a smaller surface area than activated carbon but a greater adsorption capacity. Surface area is not the only factor that influences the adsorption process. The presence of Fe_3O_4 when it comes into contact with water will undergo hydration, producing hydroxyl groups (Fe-OH), which will interact with metal ions through electrostatic bonds or ion exchange [27].

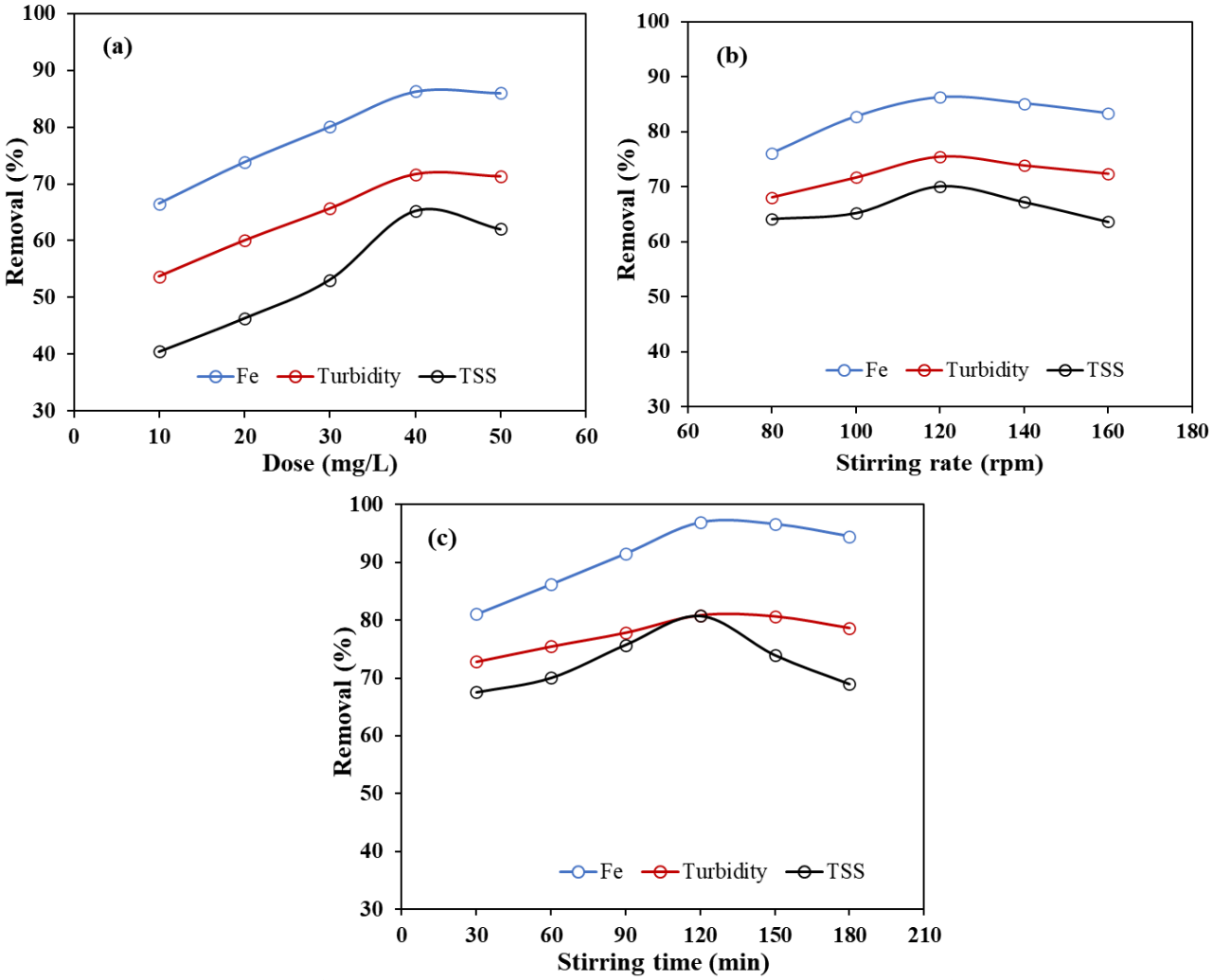

Figure 5. The effect of different parameters (a) dose, (b) stirring rate, and (c) stirring time

Table 3. Comparison of adsorption capacity between activated carbon and activated carbon-Fe_3O_4

Parameters	Enim river	After treatment	
		Activated carbon	Activated carbon-Fe_3O_4
Ion Fe (mg/L)	6.14	0.85	0.19
Turbidity (NTU)	53.57	9.37	10.26
TSS (mg/L)	1122	154	216
pH	6.23	6.74	6.86

The interaction of suspended particles with activated carbon tends to be through pores. Activated carbon has a larger surface area compared to activated carbon-Fe_3O_4. This is what makes activated carbon better at reducing turbidity and TSS. **Table** 3 shows a comparison of the reduction in Fe ion concentration, turbidity, TSS and pH changes using activated carbon and activated carbon-Fe_3O_4. The removal efficiency using activated carbon and activated carbon-Fe_3O_4 was high. Fe ions and pH concentration from processing

using activated carbon-Fe_3O_4 and pH using activated carbon meet the quality standards. This is due to the very high concentration of pollutants in the Enim river water. The reduction in TSS in this study was much greater than in other studies that used activated carbon from Cocoa husks to reduce TSS from 132 mg/L to 75.33 mg/L (30.8%) [37].

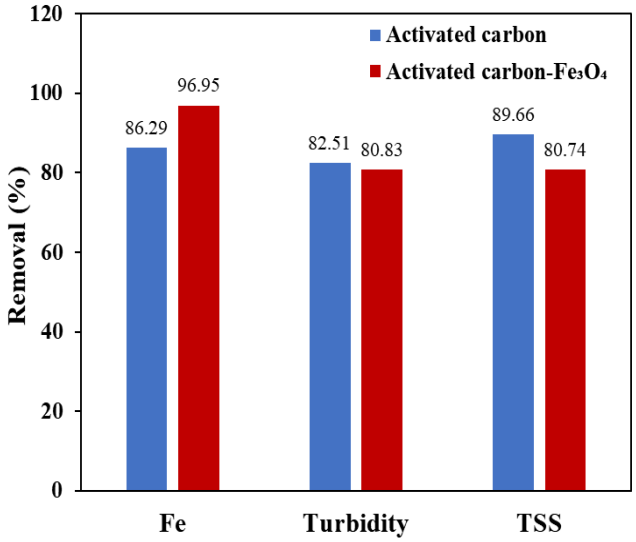

Figure 6. Comparison of removal (%) between activated carbon and activated carbon-Fe_3O_4

Adsorption kinetics

An effective adsorbent is characterized not only by its high adsorption capacity but also by the rate at which it removes contaminants. In this study, the adsorption kinetics for Fe ions were investigated. The kinetic behavior was analyzed using both the pseudo-first-order and pseudo-second-order models, as described by the following equations [33]:

$$\ln(q_e - q_t) = \ln q_e - k_1 t \quad (2)$$

$$\frac{t}{q_t} = \frac{1}{k_2 q_e^2} + \frac{t}{q_e} \quad (3)$$

Where q_e and q_t are the amount of adsorbate at equilibrium and adsorbed (mg/g) at time t. k_1 dan k_2 are the pseudo-first-order adsorption rate constant (1/min) and the pseudo-second-order adsorption rate constant (g/mg.min). The correlation coefficient (R^2) is the most important parameter, which is used to confirm the application of the model [38]. **Figure 7** shows the adsorption kinetics of activated carbon-Fe_3O_4 towards Fe ions.

It appears that the R^2 values in pseudo-first-order and pseudo-second-order are not much different, both have R^2 values > 0.99. However, the R^2 value in pseudo-second-order is greater than pseudo-first-order. This indicates that the adsorption process involves chemisorption [22]. **Table 4** shows the values of the adsorption kinetic parameters.

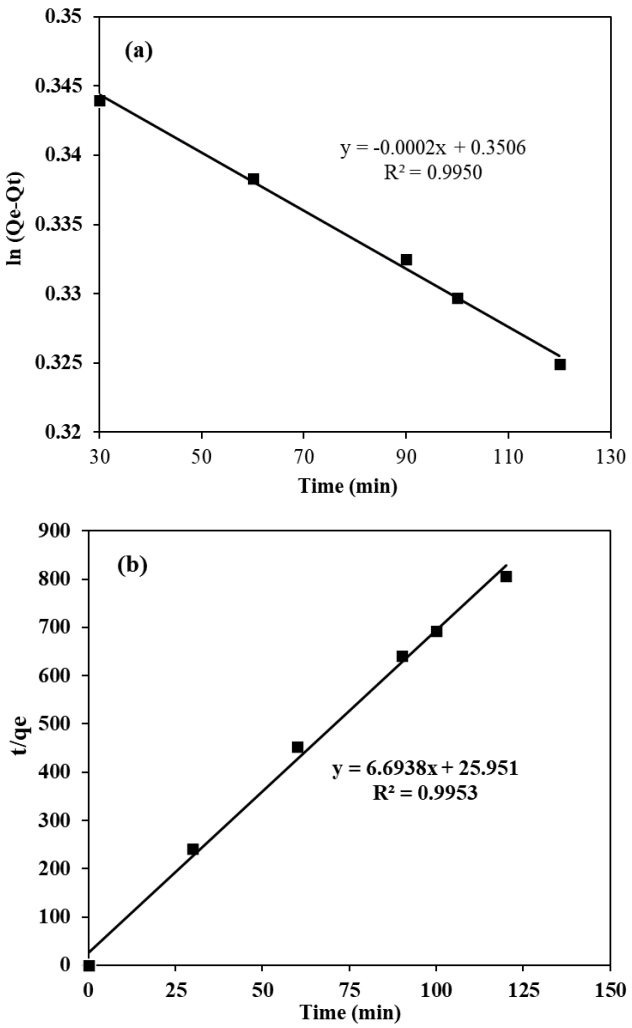

Figure 7. Adsorption kinetics of (a) pseudo-first-order and (b) pseudo-second-order for adsorption Fe ions

Table 4. The parameters of pseudo-first-order and pseudo-second-order for adsorptions Fe ions

Pseudo-first-orde		Pseudo-second-orde	
R^2	0.00508	R^2	0.9953
q_e (mg/g)	1.430	q_e (mg/g)	0.149
k_1 (min^{-1})	0.0002	k_2 ($g.mg^{-1}.min^{-1}$	1.7266

FTIR analysis before and after adsorption

Figure 8 shows the FTIR spectra of activated carbon-Fe_3O_4 before and after the adsorption process. The absorption band at wavenumbers around 3300–3400 cm^{-1} is associated with –OH stretching, indicating the presence of hydroxyl groups from adsorbed water molecules. Meanwhile, the peak in the range of ~1580–1620 cm^{-1} typically originates from

aromatic C=C bond vibrations, which are characteristic of activated carbon.

The peak at around 580 cm^{-1} indicates Fe–O vibrations, which are evidence of the formation of Fe_3O_4 nanoparticles within the activated carbon matrix [39]. After the adsorption process, changes in the intensity of several absorption bands occur. This indicates interactions between surface functional groups and pollutants, such as hydrogen bonding, metal coordination, or physical adsorption [40]. These changes are visible at wave numbers around 1600 cm^{-1}, where the peak intensity increases sharply compared to before adsorption.

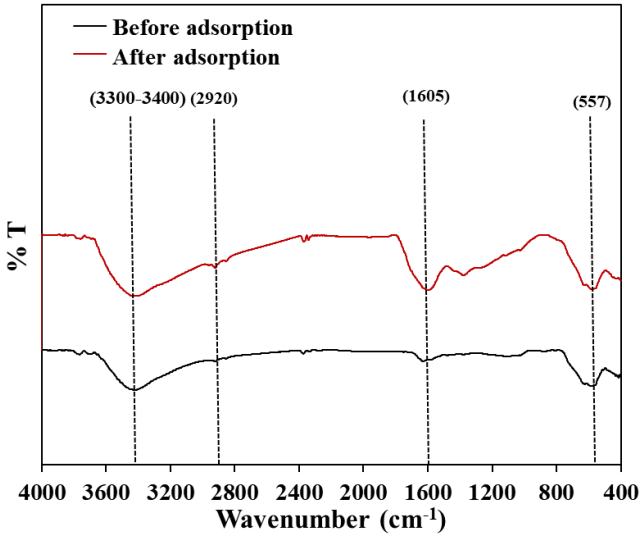

Figure 8. The FTIR spectra of activated carbon-Fe_3O_4 before and after adsorption

CONCLUSION

Activated carbon-Fe_3O_4 has been successfully synthesized using the coprecipitation method. Activated carbon is made from palm kernel shells with $ZnCl_2$ as an activator. The characterization results show that the activated carbon obtained has met SNI standards regarding moisture content, ash content, and iodine absorption capacity. The activated carbon–Fe_3O_4 composite has quite high magnetic properties, namely 68.82 emu/g, and a specific surface area reaching 334.15 m^2/g. The treatment of Enim river water using activated carbon-Fe_3O_4 showed good effectiveness in reducing the concentration of Fe ions, turbidity, and TSS, by 96.95%, 80.83%, and 80.74%, respectively. In addition, the pH value of Enim river water which was originally 6.23, increased to 6.86 after the treatment. With this performance, activated carbon-Fe_3O_4 has the potential to be further developed as an alternative adsorbent material in river water treatment, especially to produce raw water that meets the requirements for drinking water.

REFERENCES

[1] H. S. Majdi, M. S. Jaafar, and A. M. Abe, “Using KDF material to improve the performance of multi-layers filters in the reduction of chemical and biological pollutants in surface water treatment,” *South African Journal of Chemical Engineering*, vol. 28, pp. 39-45, 2019.

[2] A. Jakubaszek, “Water quality assessment after modernization of the technological system in the water treatment plant in Drzenin (Poland),” *Civil and Environmental Engineering Reports*, vol. 29(4), pp. 254-266, 2019.

[3] F. Garcia-Avila, A. Aviles-Anazco, E. Sanchez-Cordero, L. Valdiviezo-Gonzales, and M. D. T. Ordonez, “The challenge of improving the efficiency of drinking water treatment systems in rural areas facing changes in the raw water,” *South African Journal of Chemical Engineering*, vol. 37, pp. 141-149, 2021.

[4] Subroto, M. Said, E. Ibrahim, and P. L. Hariani, “Performance of coal-based activated carbon modified with $NiFe_2O_4$ for raw water treatment,” *Journal of Ecological Engineering*, vol. 26(1), 173-185, 2025.

[5] L. A, V. Govindaraj, G. Ramachandran, and P. Bermavatu, ”Removal of turbidity from lake water using novel *Chrysopogon zizanioides* and *Hemidesmus indicus*.” *Desalination and Water Treatment*,” vol. 317, pp. 1-9, 2024.

[6] P. O. Amaeh, M. A. Habila, R. Garg, C. C. Onoyima, G. O. Ihegboro, C. J. Ononamadu, R. Garg, Z. Adamu, U. J. Joel, and R. Showunmi, ”Removal of contaminants from river Jakara using iron oxide nano particles prepared from Citrullus lanatus fruit waste.” *Journal of Hazardous Materials Advances*, vol. 15, pp. 1-11, 2024.

[7] A. Chiavola, C. D. Marcantonio, M. D’Agostini, S. Leoni, and M. Lazzazzara, ”A combined experimental-modeling approach for turbidity removal optimization in a coagulation–flocculation unit of a drinking water treatment plant,” *Journal of Process Control*, vol. 130, pp. 1-10, 2023.

[8] Z. Meldha, I. Amri, M. D. T. Angkoso, Y. Jumaga, and Drastinawati, "The utilization of silica sand and clay with the addition of sawdust as raw material for manufacturing ceramic

membranes to reduce TSS and TDS levels of peat water," *Materials Today: Proceedings*, vol. 87, pp. 415-419, 2023.
[9] N. Bensitel, K. Haboubi, F. Azar, Y. El Hammoundani, A. El abdouni, C. Haboubi, F. Dimane, and A. El Kasmi, "Potential reuse of sludge from a potable water treatment plant in Al Hoceima city in northern Morocco," *Water Cycle*, vol. 4, pp. 154-162, 2023.
[10] J. Rhu, Y. Han, D. Cho, S. Kim, Y. Cho, C. Chan, J. Ahn, and I. Nam, "Practical application of PAC sludge-valorized biochars to the mitigation of methyl arsenic in wetlands," *Chemical Engineering Journal*, vol. 450(3), pp. 1-11, 2022.
[11] A. M. Dietrch, and G. A. Burlingame, "Critical review and rethinking of USEPA secondary standards for maintaining organoleptic quality of drinking water," *Environmental Science & Technology*, vol. 49(2), pp. 708-720, 2015.
[12] H. Daraei, E. Bertone, J. Awad, R. A. Steward, C. W. K. Chow, J. Duan, and J. V. Leeuwen, "A multi-analytical approach to investigate DOM dynamics and alum dose control in enhanced coagulation process using wide-ranging surface waters," *Journal of Water Process Engineering*, vol. 56, pp. 1-15, 2023.
[13] C. Cucarella, C. Montoliu, C. Hermenegildo, R. Saez, L. Manzo, M. D. Minana, and V. Felipo, "Chronic exposure to aluminum impairs neuronal glutamate-nitric oxide-cyclic GMP pathway," *Journal of Neurochemistry*, vol. 70(4), pp. 1609-1614, 1998.
[14] N. Bojanic, J. Milenkovic, D. Stojanovic, M. Milojkovic, N. Djandjic, and M. Gmiijovic, "Pathophysiological mechanisms of aluminium toxicity," *Acta Medica Medianae*, vol. 59(1), pp. 100-109, 2020.
[15] S. Mashhadi, R. Sohrabi, H. Javadian, N. Ghasemi, I. Tyadi, S. Agarwal, and V. K. Gupta, "Rapid removal of Hg (II) from aqueous solution by rice straw activated carbon prepared by microwave-assisted H_2SO_4 activation: Kinetic, isotherm and thermodynamic studies," *Journal of Molecular Liquids*, vol. 215, pp. 144-153, 2016.
[16] E. M. Mistar, T. Alfatah, and M. D. Supardan, "Synthesis and characterization of activated carbon from Bambusa vulgaris striata using two-step KOH activation," *Journal of Materials Research and Technology*, vol. 9(3), pp. 6278-6286, 2020.
[17] K. K. Kuok, P. C. Chiu, Md. R. Rahman, M. Y. Chin, and N. K. B. Bakri, "Sustainable bamboo and coconut shell activated carbon for purifying river water on Borneo Islan," *Waste Management Bulletin*, vol. 2, pp. 39-48, 2024.
[18] U. D. Hamza, N. S. Nasri, N. S. Amin, J. Mohammed, and H. M. Zain, "Characteristics of oil palm shell biochar and activated carbon prepared at different carbonization times," *Desalination and Water Treatment*, vol. 57, pp. 7999-8006, 2016.
[19] A. C. Lua, "A comparative study of the pore characteristics and phenol adsorption performance of activated carbons prepared from oil-palm shell wastes by steam and combined steam-chemical activation." *Green Chemical Engineering*, vol. 5, pp. 85-96, 2024.
[20] K. Jasri, A. S. Abdulhameed, A. H. Jawad, Z. A. Al-Othman, T. A. Yousef, and O. K. Al Duaij, "Mesoporous activated carbon produced from mixed wastes of oil palm frond and palm kernel shell using microwave radiation-assisted K_2CO_3 activation for methylene blue dye removal: Optimization by response surface methodology," *Diamond & Related Materials*, vol. 131, pp. 1-12, 2023.
[21] N. A. El-Sheeta, M. E. Goher, M. G. A. El-Moghny, and M. S. El-Deab, "Efficient elimination of Pb(II) ions from aqueous solutions using magnetic Fe_3O_4-nanoparticles/activated carbon derived from agricultural waste," *Desalination and Water Treatment*, vol. 258, pp. 241-260, 2022.
[22] S. Afshin, Y. Rashbari, M. Vosough, A. Dargahi, M. Fazizadeh, A. Behzad, and M. Yousefi, "Application of Box–Behnken design for optimizing parameters of hexavalent chromium removal from aqueous solutions using Fe_3O_4 loaded on activated carbon prepared from alga: Kinetics and equilibrium study." *Journal of Water Process Engineering*, vol. 42, pp. 1-9, 2021.
[23] M. Bagherzadeh, B. Aslibeiki, and N. Arsalani, "Preparation of Fe_3O_4/vine shoots derived activated carbon nanocomposite for improved removal of Cr(VI) from aqueous solutions," *Scientific Reports*, vol. 13, pp. 1-19, 2023.
[24] SNI 06-3730-1995. "Arang aktif teknis." Badan Standarisasi Nasional (BSN), 1995.
[25] A. H. Wazir, I. Ul Hag, A. Manan, and A. Khan, "Preparation and characterization of activated carbon from coal by chemical activation with KOH," *International Journal of Coal Preparation and Utilization*, vol. 42, pp. 1477-1488, 2020.
[26] M. Fan, T. Shao, Y. Wang, J. Sun, H. He, Y. Jiang, S. Zhang, Y. Wang, and X. Hu, "Preparation of activated carbon with recycled $ZnCl_2$ for

maximizing utilization efficiency of the activating agent and minimizing generation of liquid waste," *Chemical Engineering Journal*, vol. 500, pp. 1-18, 2024.

[27] P. L. Hariani, M. Faizal, Ridwan, Marsi, and D. Setaibudidaya, "Removal of Procion red MX-5B from songket's industrial wastewater in South Sumatra Indonesia using activated carbon-Fe_3O_4 composite," *Sustainable Environment Research*, vol. 28, pp. 158-164, 2018.

[28] C. X. M. Collave, R. J. L. Bacilio, A. E. G. Escobedo, R. F. R. Espinoza, Y. F. A. Liza, and J. M. I. Rona, "Turbidity and color removal from irrigation water, with coagulants and activated carbon, controlled by an Arduino system," *Case Studies in Chemical and Environmental Engineering*, vol. 10, pp. 1-18, 2024

[29] A. K. Badawi, R. Hassan, A. M. Alghamdi, B. Ismail, R. M. Osman, and R. S. Salama, "Advancing cobalt ferrite-supported activated carbon from orange peels for real pulp and paper mill wastewater treatment," *Desalination and Water Treatment*, vol. 318, pp. 1-10, 2024.

[30] Z. Duan, W. Zhang, M. Lu, Z. Shao, W. Huang, J. Li, Y. Li, J. Mo, Y. Li, and C. Chen, "Magnetic Fe3O4/activated carbon for combined adsorption and Fenton oxidation of 4-chlorophenol," *Carbon*, vol. 167, pp. 351-363, 2020.

[31] J. K. Alagarasan, S. Shasikal, E. R. Rene, P. Bhatt, P. Thangavelu, P. Madheswaran, S. Subramanian, D. D. Nguyen, S. W. Chang, and Moonyong Lee, "Electro-oxidation of heavy metals contaminated water using banana waste-derived activated carbon and Fe_3O_4 nanocomposites," *Environmental Research*, vol. 215, pp. 1-7, 2022.

[32] I. U. Bakara, M. D. Nurhafizah, N. Abdullah, O. O. Akinnawo, and A. Ul-Hamid, "Investigation of kinetics and thermodynamics of methylene blue dye adsorption using activated carbon derived from bamboo biomass," *Inorganic Chemistry Communications*, vol. 166, pp. 1-11, 2024.

[33] R. Foroutan, R. Mohammadi, J. Razeghi, and B. Ramavandi, "Performance of algal activated carbon/Fe_3O_4 magnetic composite for cationic dyes removal from aqueous solutions," *Algae Research*, vol. 40, pp. 1-12, 2019.

[34] WHO. "Guidelines for drinking-water quality." fourth edition, 2022.

[35] Peraturan Gubernur No. 16 tahun 2005. "Peruntukan air dan baku mutu air sungai." 2005.

[36] T. E. Oladimeji, B. O. Odunoye, F. B. Elehinafe, Oyinlola, R. Obanla, Olayemi, and A. Odunlami, "Production of activated carbon from sawdust and its efficiency in the treatment of sewage water." *Heliyon*, vol.7, pp. 1-6, 2021.

[37] K. E. V. Saltos, A. P. Á. Bravo, R. A. C. Mosquera, and M. A. Riera. "Efficiency of activated carbon derived from cocoa shells in removing pollutants from wastewater." *Journal of Ecological Engineering*, vol. 25(7), pp. 151-162, 2024.

[38] P. O. Ameh, M. A. Habila, R. Garg, C. C. Onoyima, G. O. Ihegboro, C. J. Ononamadu, R. Garg, Z. Adamu, U. J. Joel, and R. Showunmi, "Removal of contaminants from river Jakara using iron oxide nano particles prepared from *Citrullus lanatus* fruit waste," *Journal of Hazardous Materials Advances*, vol. 15, pp. 1-11, 2024.

[39] P. Chen, X. Zhang, Z. Cheng, Q. Xu, X. Zhang, Y. Liu, and F. Qiu. "Peroxymonosulfate (PMS) activated by magnetic Fe_3O_4 doped carbon quantum dots (CQDs) for degradation of Rhodamine B (RhB) under visible light: DFT calculations and mechanism analysis." *Journal of Cleaner Production*, vol. 426, pp. 1-13, 2023.

[40] W. Purwaningrum, Hasanudin, A. Rachmat, F. Riyanti, and P. L. Hariani, "Magnetic composite for efficient adsorption of iron and manganese ions from aqueous solution," *Ecological Engineering & Environmental Technology*, vol. 24(8), pp. 143-154, 2023.